Molecular bonding characteristics of Self-plasticized bamboo composites

Qiu Xue[1], Wanxi Peng[1,2]* and Makoto Ohkoshi[2]*
[1]School of Materials Science and Engineering, Central South University of Forestry and Technology, Changsha, China
[2]Lab biomaterials Science, Kyoto Prefectural University, Kyoto, Japan

Abstract: Bamboo biomass fibers were gradually separated, prepared, and then self-plasticized for immune composites. The molecular bonding characteristics of the self-plasticized bamboo composites were investigated by Fourier transform infrared spectroscopy (FT-IR), nuclear magnetic resonance spectroscopy (NMR), and thermo gravimetric analysis (TG). The important results were as follows. (1) During self-plasticizing of bamboo biomass, the cross-linking between celluloses mainly depended on carboxylic acid anhydrides and carboxylic acid esters, that between cellulose and lignin depended on carboxylic acid esters and C=O groups of aliphatic hydrocarbons, and that of hemi cellulose had a ether bond and ester bond bridging effect between lignin and cellulose. The cross-linking effects of hemi cellulose, lignin, and cellulose could be stacked and coupled. (2) After self-plasticization, the crystallinity of the lingo cellulosic biomass, lignin cellulose, and cellulose were increased by 5.8%, 2.28%, and 11.67%, respectively. While the TG curves of all samples were basically similar in shape, the weight loss rate turning points of the self-plasticized samples were delayed compared with those of the bamboo biomass fibers. This result demonstrated that the molecular integration of the bamboo biomass was increased after self-plasticization, and confirmed that bond cross-linking between the hemi cellulose, lignin and cellulose of the bamboo biomass had occurred.

Keywords: Molecular bond; bamboo self-plasticizing; ligno cellulosic biomass; lignin cellulose; cellulose.

INTRODUCTION

The fine recombination of wooden fibers, key for the manufacture of wood-based panels and papermaking, has been the focus of academic research in wood science. The recombination of wooden fibers began in 105 A.D. when Cai Lun invented papermaking. Wet-process fiberboard dominated after the invention of phenol formaldehyde resin and urea formaldehyde resin, but was replaced by dry-process fiberboard because its manufacture produces less wastewater and residual pollution (Turk *et al.*, 2007; Burton *et al.*, 2011). However, dry-process fiberboard, the manufacture of which requires large amounts of phenol formaldehyde resin or urea formaldehyde resin, releases a large number of indoor pollutants such as formaldehyde and free phenol, which seriously damage the human liver (Rong *et al.*, 2010). To eliminate indoor pollutants such as formaldehyde, increasing numbers of scholars have studied how to glue wooden fibers without adhesives by physical, chemical, or biological methods. Since Tischer began such research, wooden fibers have been, for example, treated to increase their free radicals and then hot-press glued (Roger *et al*., 2008; Bowang *et al.*, 2010), treated with high-pressure steam and glued using bonding-capable hemicellulose (Widyorini *et al*., 2005), and activated for self-gluing by enzymes (Muller *et al*., 2009; Catalina *et al*, 2011). The six methods of gluing wooden fibers without adhesive identified so far are oxidation, free radicals, acid catalyzed polycondensation, alkali solution activation, natural material transformation, and enzyme activation. However, these methods involve cumbersome processes, are inefficient, or result in insufficient binding strength and other defects, and have therefore not seen large-scale industrial application.

The plasticizing of wood (including bamboo) has also been identified as an effective bonding method to eliminate the indoor pollutants, and has two approaches. The first relies on the plastic properties of resin, into which the wood or bamboo is immersed and then plasticized. Wood treated in this way has been reported to show good plasticization due to its high porosity and easy absorption of resin, however, bamboo showed poor plasticization due to its dense texture which hindered resin absorption (Kaufman *et al.*, 2010). The second approach involves the uniform mixing of plastic and timber (or bamboo), followed by a shaping process such as extrusion, molding, or injection to obtain a wood-plastic or bamboo-plastic composite material (Hung *et al.*, 2012; Hung *et al.*, 2010). However, the poor interfacial convergence of bamboo-plastic composite material made it unsatisfactory in industrial applications. At the same time, the amount of added plastic, the price of which was 2–5 times that of wood or bamboo, required was at least 30%, resulting in a substantially increased cost and decreased added value of bamboo-plastic products (Xu *et al.*, 2008; Jian *et al*., 2012). To improve the plasticization of bamboo and decrease plasticizing cost it has therefore been necessary to carry out pivotal research on the self-plasticization of bamboo cell walls. In this work, bamboo

**Corresponding authors:* e-mail: pengwanxi@163.com; mohkoshi@kpu.ac.jp

biomass was extracted, separated and then self-plasticized for immune composites, and the molecular bonding characteristics of the resulting self-plasticized bamboo samples were proposed and investigated by nuclear magnetic resonance (NMR), Fourier transform infrared spectroscopy (FT-IR) and thermo gravimetric analysis (TG).

MATERIALS AND METHODS

Test materials

Two 7-year-old *Phyllostachys heterocycla* were collected from the forest farm of Longshan County, Hunan Province, P.R. China. Sample chips were ground from the fresh material and dried to absolute dry weight at 105°C. 40-200 mesh powders were sieved out from the samples using a AS200 Sieving Instrument (Retsch, USA). Benzene, ethanol, acetic acid (100%), hydrogen peroxide (30%), and sodium hydroxide (analytical grade) were used in the subsequent experiments. Cotton bags and cotton were immersed in benzene/ethanol solution for 24 h ($V_{ethanol}$ /$V_{benzene}$ =2).

Preparation of bamboo biomass fibers

Lignocellulosic biomass preparation

100g portions of the bamboo powder were parceled using cotton bags and tied using cotton thread. Extraction was carried out in 300 mL benzene/ethanol solution in a large-caliber Soxhlet at 80-85°C for 6 h. After extraction, samples were baked to absolute dryness at 55°C under negative 0.01MPa. The total weight of the treated bamboo powder was 1000g. The sample ID was Qm11.

Lignincellulose preparation

750g lignocellulosic biomass was treated in 17.5% sodium hydroxide solution at 20-25°C for 24 h according to $V_{sodium\ hydroxide\ solution}/V_{Lignocellulosic\ biomass}$ =20. After treatment and filtration, the samples were neutralized using acetic acid and baked to absolute dryness at 55°C under negative 0.01 MPa. The sample ID was Qm21.

Cellulose preparation

350g lignincellulose was treated in acetic acid-hydrogen peroxide solution at 20-25°C for 24 h according to $V_{acetic\ acid\ -hydrogen\ peroxide\ solution}/V_{Lignincellulose}$ =10. The mixed solution was stirred at 1 h intervals. After treatment and filtration, the samples were neutralized using sodium hydroxide and baked to absolute dryness at 55°C under negative 0.01 MPa. The sample ID was Qm31. The acetic acid-hydrogen peroxide solution was mixed according to $V_{acetic\ acid}/V_{hydrogen\ peroxide}$ =1.

Preparation of self-plasticized samples

One hundred and fifty grams of sample powder was placed in a mold. The self-plasticizing conditions were programmed as follows: The samples were rapidly heated from room temperature to 160°C, and the pressure was rapidly increased from 0 MPa to 65 MPa. They were then molded at 160°C under 65 MPa for 30 min, cooled to room temperature, and the pressure was released. The self-plasticized samples of lingo cellulosic biomass, lignin cellulose, and cellulose were named Qm12, Qm22 and Qm32, respectively. The samples were ground, and the 200mesh powder was sieved out and baked to absolute dryness under 0.009 MPa at 55°C.

FT-IR analysis

There FT-IR spectra of above samples were obtained on a FT-IR spectrophotometer (IR100) using KBr discs containing 1% finely ground sample.

NMR analysis

The 200mesh powder was ground in a rotary mill filled with dense 4 mm ZrO_2 balls. And solid-state NMR spectra were measured at 25°C on a Bruker 400M-AV-III spectrometer. The number of scans was 5000. Sampling was carried out using the standard Bruker CP-MAS program, CP-MAS acquisition mode, a relaxation time of 2 s, a cross-polarization pulse program matching the detection time of 1 ms and a rotational frequency of 5000 Hz. The chemical shift was corrected using the 176 ppm glycine carbonyl group.

TG analysis

TG spectra were measured on a TG20 Thermal gravimetric analyzer (NETZSCH, Germany) using a carrier gas (N_2) velocity of 40mL/min at 5, 15, 25 and 35°C/min from room temperature to 250°C. Less than 10 mg of each sample was analyzed. The weight loss rates were obtained by automatic data collection systems.

RESULTS

Fig. 1 displays the FT-IR spectra of cellulose (Qm31) and its self-plasticized sample (Qm32).

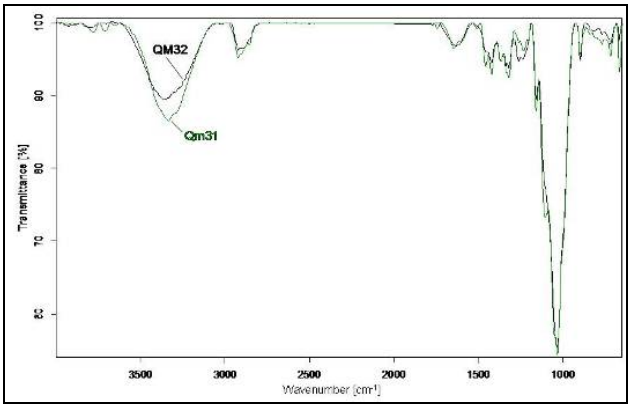

Fig. 1: FT-IR spectra of Qm31 and Qm32 samples of bamboo cellulose

There were many peaks in the ^{13}C-NMR spectrum of cellulose (shown in fig. 2). And fig.3 was ^{13}C-NMR spectrum of Qm32 sample of bamboo cellulose

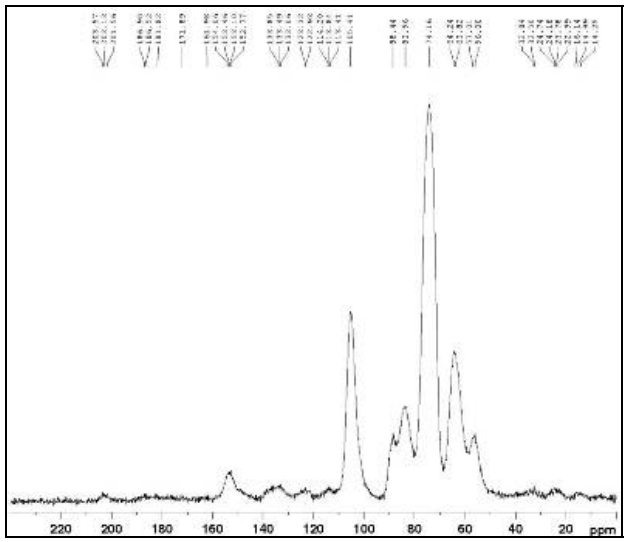

Fig. 2: ^{13}C-NMR spectrum of Qm31 sample of bamboo cellulose

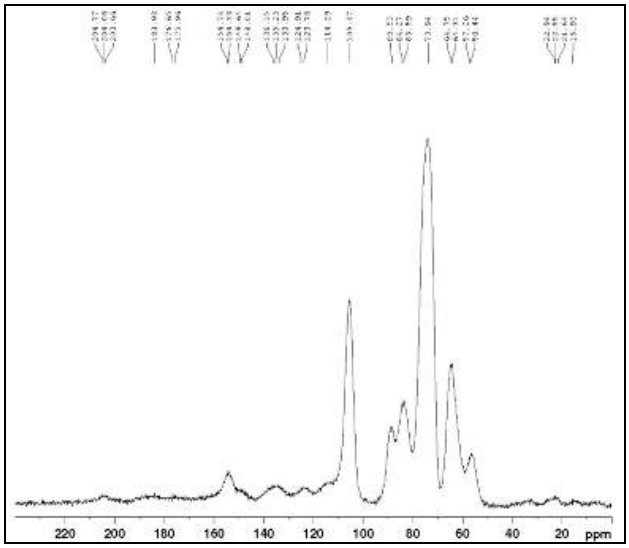

Fig. 3: ^{13}C-NMR spectrum of Qm32 sample of bamboo cellulose

Fig. 4 shows the FT-IR spectra of lignin cellulose (Qm21) and its self-plasticized sample (Qm22). There were many peaks in **^{13}C**-NMR spectrum of lignin cellulose (fig. 5). And fig. 6 was the ^{13}C-NMR spectrum of Qm22 sample of bamboo lignin cellulose

Fig. 7 shows the FT-IR spectra of lignocellulosic biomass (Qm11) and its self-plasticized sample (Qm12). There were many peaks in ^{13}C-NMR spectrum of the lingo cellulosic biomass (fig. 8).

Fig. 9 was the ^{13}C-NMR spectrum of Qm12 sample of bamboo lingo cellulosic biomass. And fig. 10: FT-IR spectra of Qm12, Qm22, and Qm32 samples.

Fig. 11-13 display the TG curves of lingo cellulosic biomass, lignin cellulose, cellulose, and their self-plasticized samples.

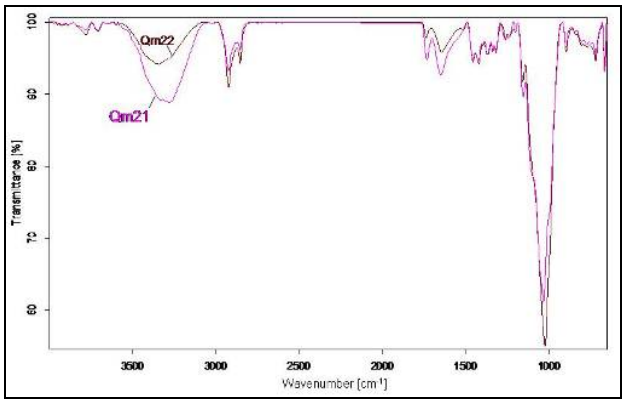

Fig. 4: FT-IR spectra of Qm21 and Qm22 samples of bamboo lignin cellulose

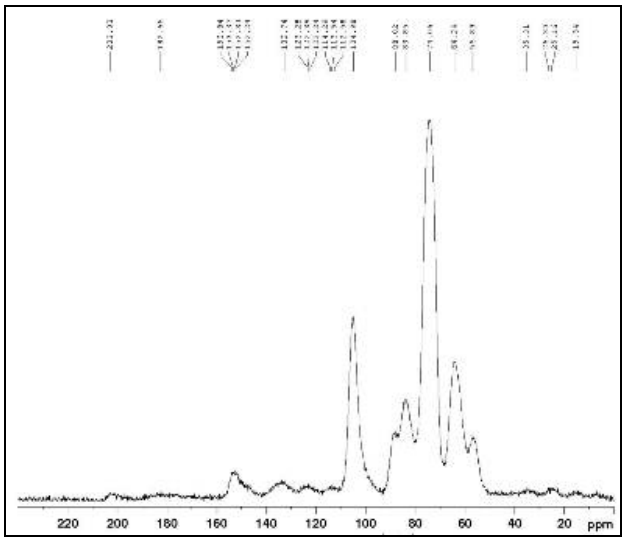

Fig. 5: ^{13}C-NMR spectrum of Qm21 sample of bamboo lignin cellulose

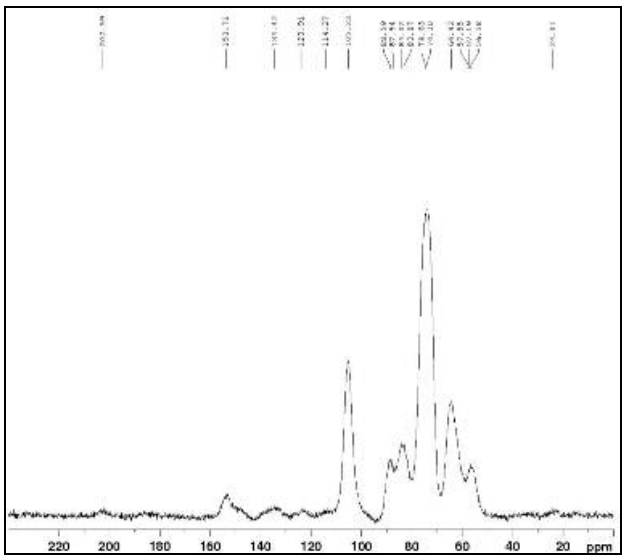

Fig. 6: ^{13}C-NMR spectrum of Qm22 sample of bamboo lignin cellulose

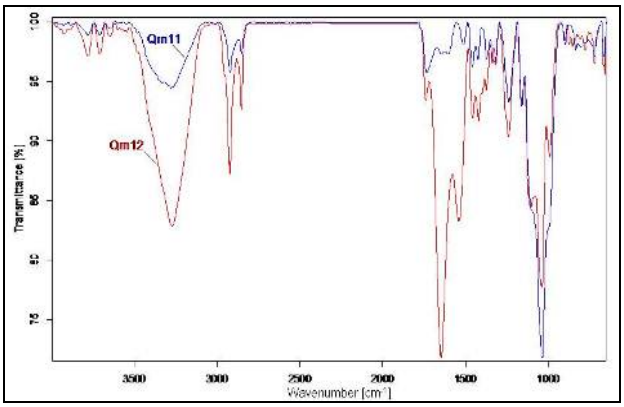

Fig. 7: FT-IR spectra of Qm11 and Qm12 samples of bamboo lingo cellulosic biomass

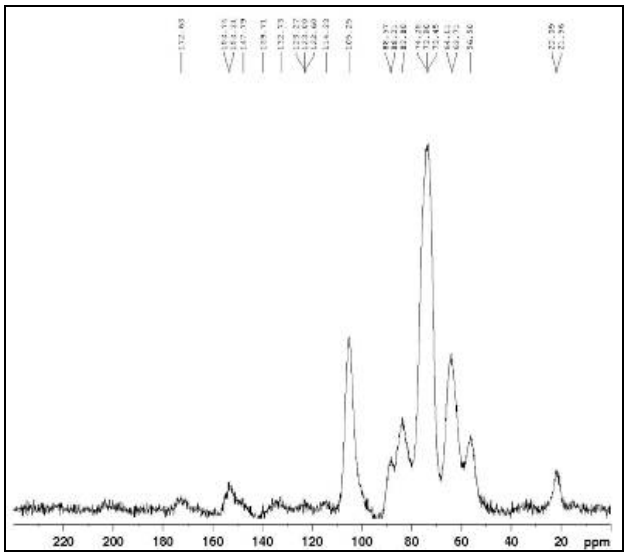

Fig. 8: ^{13}C-NMR spectrum of Qm11 sample of bamboo lingo cellulosic biomass

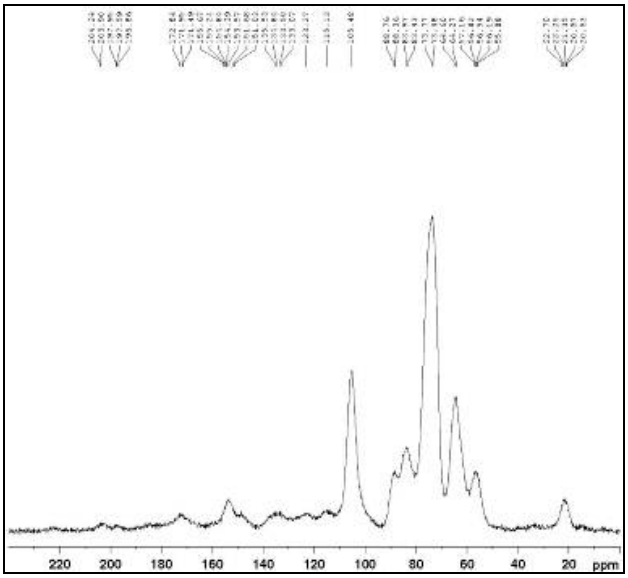

Fig. 9: ^{13}C-NMR spectrum of Qm12 sample of bamboo lingo cellulosic biomass

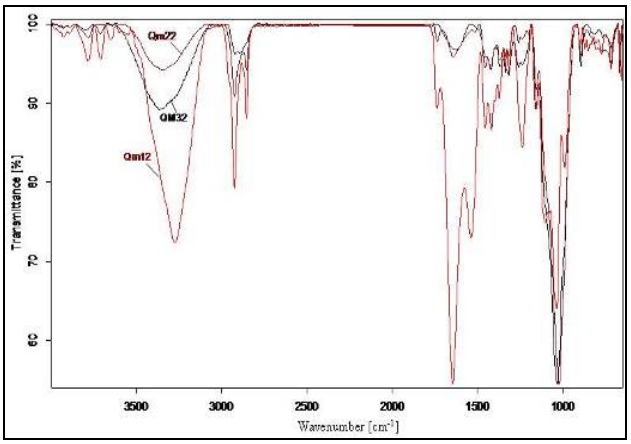

Fig. 10: FT-IR spectra of Qm12, Qm22, and Qm32 samples

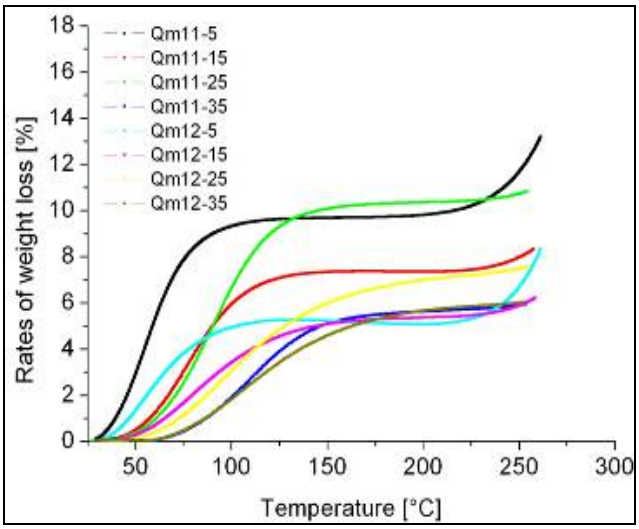

Fig. 11: TG curves of Qm11 and Qm12 samples of bamboo lingo cellulosic biomass

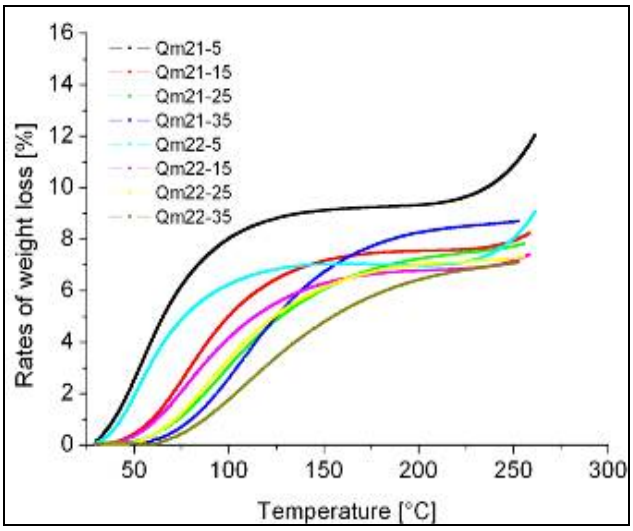

Fig. 12: TG curves of Qm21 and Qm22 samples of bamboo lignin cellulose

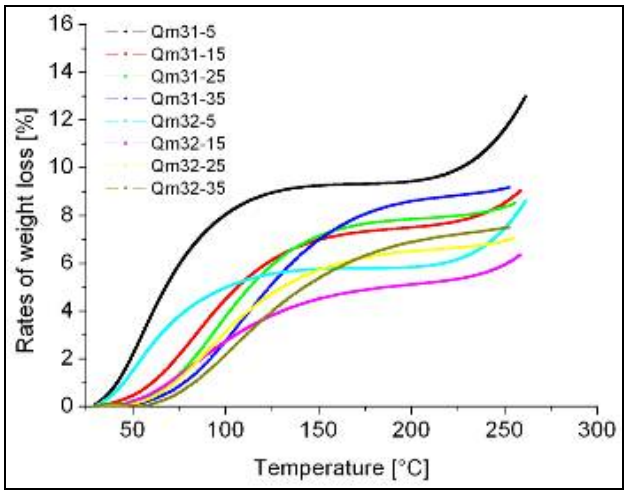

Fig. 13: TG curves of Qm31 and Qm32 samples of bamboo lignin cellulose

Using the above solid NMR spectra, crystallinity (CrI) was the ratio of the percentages of crystallized regions I_C (89 ppm, C-4) and amorphous regions I_a (84 ppm, C-4) of the cellulose in the bamboo biomass (Formula 1). The calculated results are shown in table 1. Table 2 was Turning points of weight loss rates of all the samples.

$$CrI = \frac{Ic}{Ic + Ia} \quad (1)$$

Table 1: Crystallinity of all samples (%)

Bamboo biomass	Non-plasticized samples	Plasticized samples	Difference
Lignocellulosic biomass	28.82	40.49	11.67
Lignincellulose	36.63	38.91	2.28
Cellulose	37.87	43.67	5.8

ANALYSIS

Bonding characteristics of self-plasticized cellulose

In the FT-IR spectra of Qm31, the peaks of 3333 cm^{-1}, 2921 cm^{-1}, 1744 cm^{-1}, 1237 cm^{-1}, 1159 cm^{-1}, 1036 cm^{-1}, 897 cm^{-1}, 833 cm^{-1} were assigned to the stretching vibrations of -OH, -CH_2-, non-conjugated C=O, C-O or conjugated C=O , C-O or C-C, C-O-C, and cellulose β-bonds, respectively. Two sharp bonds at 1457cm^{-1} and 1365cm^{-1} represented the methylene and methyl bending vibrations, respectively. The peak at 1104cm^{-1} was assigned to Ar-OH and secondary alcohol C-O stretching vibrations. Three sharp bonds at 1646cm^{-1}, 1509cm^{-1} and 1422cm^{-1} were the characteristic peaks of lignin. This meant that there was a small amount of lignin present in the cellulose as a result of the acetic acid-hydrogen peroxide method not achieving complete delignification of the lignin cellulose.

There were many differences in the FT-IR spectra of sample Qm32 compared with that of sample Qm31. The transmittance of the -CH_3 stretching vibration was lower after self-plasticization, while all others were larger. The peaks assigned to C-O-C, -CH_2-, Ar-OH and secondary alcohol C-O disappeared, while a peak attributable to OH plane deformation vibration at appeared 1338 cm^{-1}. This result indicated that dehydration or etherification of the cellulose occurred and that the β-OH of the amorphous regions were broken.

The peaks at 201-203 ppm, 186 ppm and 181 ppm, 171 ppm, 152-154ppm, 133 ppm, 122-123ppm, 113-114 ppm, 105 ppm, 88 ppm, 83 ppm, 74 ppm, 63-64 ppm, 56-57ppm, 32 ppm, 22-24ppm, and 14-16ppm were assigned to C=O of ketone, C=O of aldehyde or acid, C=O of ether bonds, C3/C5 of etherified syringyl, C-4 of etherified syringyl, C-6 of etherified syringyl, C-5 of guaiacyl, C-1 of cellulose, C-4 (crystalline regions) of cellulose, C-4 (amorphous regions) of cellulose, C-3/C-2/C-5 of cellulose, C-6 of cellulose, methoxy of lignin, methylene

Table 2: Turning points of weight loss rates of all the samples

Temperature	Qm31-5	Qm31-15	Qm31-25	Qm31-35	Qm32-5	Qm32-15	Qm12-25	Qm12-35
100°C	8.02	4.47	3.76	2.70	4.96	2.72	3.10	2.16
200°C	9.41	7.49	7.84	8.59	5.82	5.10	6.50	6.87
250°C	11.59	8.51	8.34	9.11	7.43	5.96	6.93	7.47
Temperature	Qm21-5	Qm21-15	Qm21-25	Qm21-35	Qm22-5	Qm22-15	Qm22-25	Qm22-35
100°C	8.01	5.01	3.04	2.56	6.23	4.15	3.34	1.75
200°C	9.31	7.53	7.22	8.25	6.97	6.76	7.00	6.41
250°C	10.85	7.92	7.72	8.67	8.01	7.14	7.24	7.05
Temperature	Qm11-5	Qm11-15	Qm11-25	Qm11-35	Qm12-5	Qm12-15	Qm12-25	Qm12-35
100°C	9.32	5.93	6.64	1.89	4.93	3.42	3.05	1.83
200°C	9.81	7.35	10.35	5.62	5.07	5.36	6.98	5.65
250°C	11.66	7.97	10.73	5.89	6.66	5.88	7.47	6.00

of aliphatic hydrocarbons, methyl in acetyl group, and C in unsaturated lignin side chains, respectively. It was further confirmed that there a small amount of lignin was present in the cellulose. Compared with the ^{13}C-NMR spectrum of sample Qm31, a new peak assignable to C=O of carboxylic acid anhydride or carboxylic acid esters appeared at 149 ppm in the ^{13}C-NMR Spectrum of sample Qm32, while the peak assigned to methylene of aliphatic hydrocarbons disappeared. This demonstrated that the cellulose molecule chains of amorphous regions were broken by oxidation or pyrolysis reactions.

On the basis of the results of the ^{13}C-NMR and FTIR analyses, *β*-OH and the cellulose molecule chains of the amorphous regions were broken but OH plane deformation and carboxylic acid anhydrides or carboxylic acid esters were created after self-plasticization. This caused amorphous regions of the cellulose to be reduced and its crystallinity increased, as shown in table 1. The above evidence illustrates that cross-linking reactions took place between cellulose molecule chains and amorphous regions of the cellulose through new carboxylic acid anhydrides or carboxylic acid ester groups.

Bonding characteristics of self-plasticized lignin cellulose

In the FT-IR spectra of Qm21, the peaks at 3280 cm^{-1}, 2923 cm^{-1}, 2653 cm^{-1}, 1733 cm^{-1}, 1261 cm^{-1}, 1156 cm^{-1}, 1034 cm^{-1}, and 897 cm^{-1} were due to the stretching vibrations of -OH, -CH_2-, -CH_3, non-conjugated C=O, C-O or conjugated C=O, C-O or C-C, C-O-C, and cellulose *β*-bonds, respectively. Two sharp peaks at 1456 cm^{-1} and 1373 cm^{-1} represent the methylene and methyl bending vibrations, respectively. Two sharp peaks at 1646 cm^{-1} and 1424 cm^{-1} were the characteristic peaks of lignin. The peaks at 1338 cm^{-1} and 1316 cm^{-1} were assignable to the condensation syringyl bond stretching vibration.

There were many differences in the FT-IR spectra of Qm22 compared with that of Qm21.The transmittances of -OH, non-conjugated C=O, C-O-C, condensation syringyl, and the cellulose *β*-bond stretching vibration were all larger after self-plasticization. However, the transmittances of the C-O and conjugated C=O stretching vibrations, and -CH_2- and -CH_3 bending vibrations were all-lower. It could be further deduced from the observed results that non-conjugated C=O, -OH, C-O-C, the cellulose *β*-bonds and the lignin and cellulose benzene rings were broken, and C-O, C-C, -CH_2-, CH_3 and conjugated C=O groups grew in number.

The peaks at 203 ppm, 182 ppm, 152-153ppm, 132 ppm, 122-123 ppm, 112-114 ppm, 104 ppm, 88 ppm, 83 ppm, 74 ppm, 64 ppm, 56 ppm, 35 ppm, 25-26 ppm, and 15 ppm were assigned to C=O of ketone, C=O of aldehyde or acid, C3/C5 of etherified syringyl, C-4 of etherified syringyl, C-6 of etherified syringyl, C-5 of guaiacyl, C-1 of cellulose, C-4 (crystalline regions) of cellulose, C-4 (amorphous regions) of cellulose, C-3/C-2/C-5 of cellulose, C-6 of cellulose, methoxy of lignin, methylene of aliphatic hydrocarbons, methyl in acetyl group, and C in unsaturated side chain of lignin, respectively. The ^{13}C-NMR spectrum of self-plasticized lignin cellulose (fig. 6) was significantly different to that of lignin cellulose. After self-plasticization, the peaks of aldehyde or acid C=O disappeared, meaning that these groups may have been oxidized and underwent addition, dehydration, or esterification reactions. Furthermore, aliphatic hydrocarbon methylene, acetyl group methyl, and unsaturated lignin side-chain carbon also disappeared, indicating that part of the -CH_2-, C-C, and -CH_3 bonds in the lignin and cellulose were broken by oxidation and pyrolysis reactions.

Based on the results of the ^{13}C-NMR and FTIR analyses, aldehyde or acid C=O and unsaturated lignin side chains were broken and C-O, C-C, -CH_2-, CH_3 and conjugated C=O groups grew in number. Besides the reaction between cellulose molecules, bamboo lignin cellulose self-plasticization led to a decrease in the number of lignin molecule side chains, and some inserted into amorphous regions of the cellulose to create a molecular mosaic effect under the high pressure. Consequently, interactive cross-linking occurred between the cellulose and lignin through new carboxylic acid esters and aliphatic hydrocarbon O=C groups.

Bonding characteristics of self-plasticized lignocellulosic biomass

In the FT-IR spectra of Qm11, the peaks at 3270 cm^{-1}, 2920 cm^{-1}, 2850 cm^{-1}, 1734 cm^{-1}, 1237 cm^{-1}, 1159 cm^{-1}, 1036 cm^{-1}, 897 cm^{-1}, 833 cm^{-1} were assigned to the stretching vibration of hydroxyl (-OH), methylene(-CH_2), methyl(-CH_3), non-conjugated carbonyl groups (non-conjugated C=O), carbon single-bonded oxygen (C-O) or conjugated carbonyl groups (conjugated C=O), carbon single-bonded oxygen (C-O) or carbon-carbon single bonds (C-C), ether bonds (C-O-C), polysaccharide *β*-bonds, and polysaccharide *α*-bonds, respectively. Two sharp peaks at 1458 cm^{-1} and 1370 cm^{-1} represented the methylene and methyl bending vibrations, respectively. Three sharp signals at 1600 cm^{-1}, 1510 cm^{-1}, and 1422 cm^{-1} were the characteristic peaks of lignin. The peak at 1329 cm^{-1} was assignable to the condensation syringyl stretching vibration.

There were many differences in the FT-IR spectra of Qm12 compared with that of Qm11.The transmittances of –OH, -CH_2-, -CH_3, non-conjugated C=O stretching vibrations and the -CH_2- and -CH_3 bending vibrations were all lower after self-plasticization. However, the transmittances of C-O or C-C, C-O-C, the polysaccharide *β*-bond, and the *α*-bond stretching vibrations were all

larger, and new peaks appeared at 1105 cm^{-1}, 1036 cm^{-1}, 990 cm^{-1}. Some significant changes occurred in the characteristic peaks of lignin; the peak at 1600 cm^{-1} disappeared and the transmittances of the other two peaks were lower. Meanwhile, a new peak assigned to the conjugated C=O stretching vibration appeared at 1647 cm^{-1}, and the transmittance of the condensation syringyl bending vibration was lower. It could be further deduced from the observed results that non-conjugated C=O bonds in the lignin were broken and generated some stable chemical bonds such as C-O, C-C, or conjugated C=O. Thus, during the self-plasticization of the lingo cellulosic biomass, its lignin, cellulose, and hemi cellulose reacted by dehydration, thermal aging, thermal degradation, and so on, resulting in the breaking of unstable groups such as C-O-C, non-conjugated C=O and C-O of O=C-O-C and generation stable chemical bonds. Cross-linking reactions between lignin, cellulose and hemi cellulose may have occurred simultaneously.

The peak assignable to ester bond C=O was located at 172 ppm, and those of the benzene ring in lignin occurred in the range 110-160 ppm; namely 153 ppm for C3/C5 of etherified syringyl, 132 ppm C-4 of etherified syringyl, 114 ppm C-5 of guaiacyl, 147 ppm non-etherified syringyl, 139 ppm benzene ring of lignin, 123-122 ppm C-6 of benzene ring in oxidized guaiacyl. The signal of cellulose C-1 appeared at 105 ppm, that of C-4 (crystalline regions) at 88 ppm, C-4 (amorphous regions) at 83 ppm, C-3, C-2 and C-5 at 73-74 ppm, and C-6 at 63-64ppm. The signal peak of lignin methoxy lay at 56 ppm. The signal peak at 21-22-ppm was assigned to acetyl group methyl.

The density of the lingo cellulosic biomass increased after self-plasticization, and the spatial separation between the three components of the lingo cellulosic biomass became smaller. This caused the signal peaks of the Qm12 sample to be more conspicuous than those of the Qm11 sample (fig. 8 and fig. 9). A new peak assigned to ketone C=O appeared at 203-204 ppm, meaning that oxidation of lignin side chains occurred during the self-plasticization of the lignocellulosic biomass. The other peaks of lignin and ester bonds did not change significantly. The peak assigned to cellulose C-1 shifted from 105.2 ppm to 105.4 ppm, cause by increases in hydrogen bonding and the amount of crystalline regions self-plasticization. This could also be seen from the peak at 3200 cm^{-1} in the FT-IR spectra of Qm11 and Qm12. Thus, side-chain oxidation of lignin and hydrogen bond enrichment arose during lignocellulosic biomass self-plasticization.

According to the results of the ^{13}C-NMR and FTIR analyses, the characteristic peaks of lignin disappeared but those of C-O or C-C, C-O-C, polysaccharide β-bonds and α-bonds intensified, and of conjugated α/β-ketone C=O, and ether, lipid and alcohol C-O were created, specifically the amount of hydrogen bonds increased after self-plasticization. Besides the reactions in self-plasticized lignin cellulose and cellulose, the bamboo lingo cellulosic biomass underwent hydrolytic and thermal degradation reactions to create -C=O, -C-OH and -COOH, resulting in the increase of the crystallinity of the cellulose (table 1). These newly created groups in the lignin, cellulose, and hemi cellulose underwent cross-reactions. In addition, some of Ar rings in lignin were also broken. As a result, the hemi cellulose exhibited ether bonds and an ester bond bridging effect occurred between the lignin and cellulose of the bamboo lingo cellulosic biomass.

Effect of bamboo self-plasticizing on crystallinity

Crystallinity is an important structural parameter of supramolecular cellulose that influences not only the physical and chemical properties of cellulose but those of bamboo biomass. Table 1 shows that the crystallinity of lingo cellulosic biomass, lignin cellulose, and cellulose increased by 5.8%, 2.28%, and 11.67%, respectively, after self-plasticization. There are two kinds of water (free water and combined water) present in bamboo cell walls. If only heat or low pressure is applied to bamboo biomass, only free water would evaporate from the bamboo cell walls. Treatment of bamboo biomass by heat and high pressure first caused the free water to evaporate from the bamboo cell wall, and part of the combined water dissociated from the amorphous cellulose regions. Simultaneously, the space between cellulose molecule chains became very small, resulting in chemical bonding reactions and hydrogen bonding between cellulose molecules. The amount of hydrogen bonds decreased in the amorphous cellulose regions, which decreased the distance between the C-4 of cellulose. Thus, crystallinity was increased. Fig. 10 shows that the transmittance of the -OH peaks gradually decreased among the self-plasticized samples of lignin cellulose, cellulose and lingo cellulosic biomass, indicating that hemi cellulose had a significant influence on the crystallinity of the bamboo biomass. Thus lignin, cellulose, and hemi cellulose might all contribute to the self-plasticization of bamboo biomass.

TG analysis of bamboo biomass

Between 0-100°C, water evaporated from the samples and their weight reduced. The weight loss rates of the self-plasticized samples were lower than those of the lingo cellulosic biomass, lignin cellulose and cellulose because the structures of the self-plasticized samples were much closer together than those of the untreated samples. Between 100-200°C, the combined water began to dissociate, resulting in the weight loss rates of the self-plasticized samples becoming the same as those of the lingo cellulosic biomass, lignin cellulose and cellulose. Above 200°C, lingo cellulosic biomass, lignin cellulose, cellulose and their self-plasticized samples began undergo pyrolysis, resulting in the rates of weight loss becoming large. Figs. 11-13 also show that there were some

similarities and differences among the TG curves of the lingo cellulosic biomass, lignin cellulose, cellulose and their self-plasticized samples. The weight loss rates observed at 25°C/min of the untreated samples were very similar to those of the self-plasticized samples, but at 5°C/min large differences between the weight loss rates of the untreated samples and the self-plasticized samples were observed. While the shapes of both sets of TG curves were basically similar, the turning points of the weight loss rates of the self-plasticized samples were delayed compared with those of the corresponding untreated samples (table 2). This was further proof that the molecular integration of the bamboo biomass increased after self-plasticization due to the creation of molecular compounds between lignin, cellulose, and hemi cellulose.

CONCLUSIONS

FT-IR and ^{13}C-NMR results demonstrated that lingo cellulosic biomass, lignin cellulose, and cellulose exhibited different bonding characteristics after self-plasticization. Cross-linking reactions took place between cellulose molecule chains and amorphous cellulose regions through new carboxylic acid anhydrides or carboxylic acid esters. Interactive cross-linking reactions occurred between cellulose and lignin by new carboxylic acid esters and aliphatic hydrocarbon O=C groups. Hemi cellulose exhibited ether bond and ester bond bridging effects between the lignin and cellulose of bamboo lingo cellulosic biomass. Thus lignin, cellulose, and hemi cellulose all contributed to the self-plasticization of bamboo biomass.

Furthermore, the crystallinity of lingo cellulosic biomass, lignin cellulose, and cellulose increased by 5.8%, 2.28%, and 11.67%, respectively after self-plasticization. The TG curves of all samples were basically similar in shape, but the turning points of the weight loss rates of the self-plasticized samples were delayed in comparison with those of the untreated samples. This result was further confirmation that the molecular integration of bamboo biomass was increased by new cross-linking reactions between lignin, cellulose and hemi cellulose during self-plasticization.

ACKNOWLEDGMENTS

This work was financially supported by the National Natural Science Foundation of China (No.31170532), Program for New Century Excellent Talents in University (No. NCET-10-0170), and the Scientific Research Fund of Hunan Provincial Education Department (No. 10A131).

REFERENCES

Burton C, Bradshaw L, Agius R, Burge S, Huggins V and Fishwick D (2011). Medium-density fibreboard and occupational asthma: A case series. *Occup. Med.* (Lond) **61**(5): 357-363.

Bowang Y, Linsong K and Baozhang S (2010). The Research progress in pretreatment techniques of self-bonding composites. *J. Adv. Mater Res.,* **113**(116): 2337-2343.

Catalina Á, Benjamín R, Ovidio A, Orlando JR and Piedad G (2011). Self-bonding boards from plantain fiber bundles after enzymatic treatment: Adhesion improvement of lignocellulosic products by enzymatic Pre-Treatment. *J. Polym. Environ.,* **19**(1): 182-188.

Hung K-C, Chen Y-L and Wu J-H (2012). Natural weathering properties of acetylated bamboo plastic composites. *Polym. Degrad. Stabil.,* **97**(9): 1680-1685

Hung KC and Wu JH (2010). Mechanical and interfacial properties of plastic composite panels made from esterified bamboo particles. J. Wood Sci., **56**(3): 216-221

Jian H and Dan L (2012). Valuation on mildew-proof results of ACQ-B to bamboo. *Adv. Mater. Res.,* **580**: 517-520.

Kaufman WR, Flynn PC and Reynolds E (2010). Cuticular plasticization in the tick, Amblyomma hebraeum (Acari: Ixodidae): Possible roles of monoamines and cuticular pH. *J. Exp. Biol.,* **213**(16): 2820-2831

Muller C, Euring M and Kharazipour A (2009). Enzymatic modification of wood fibres for activating their ability of self-bonding. *Int. J. Mater. Prod. Tech.,* **36**(1-4): 189-199

Rong H, Liu Z, Wu Q, Pan D and Zheng J (2010) Formaldehyde removal by Rayon-based activated carbon fibers modified by P-aminobenzoic acid. *Cellulose,* **17**(1): 205-214.

Roger M, Rowell JD and Mc Sweeny (2008) Heat Treatments of Wood Fibers for Self-Bonding and Stabilized Fiberboards. *Mol. Cryst. Liq. Cryst.,* **483**(1): 307-332.

Turk C and Hunt JF (2007). Development of a bending stiffness model for wet process fiberboard. *Wood Fiber Sci.,* **39**(1): 196-203

Widyorini R, Xu JY and Watanabe T (2005). Chemical changes in steam-pressed kenaf core binderless particleboard. *J. Wood Sci.,* **51**: 6-32

Xu YZ, Wang CP and Chu FX (2008). Progress on technology of internal plasticization of cellulose. *Polym. Mater Sci. Eng.,* **24**(9): 19-22.